JOC The Journal of Organic Chemistry

Article

pubs.acs.org/joc

Reaction Pathway and Rate-Determining Step of the Schmidt Rearrangement/Fragmentation: A Kinetic Study

Ryo Akimoto, Takehiro Tokugawa, Yutaro Yamamoto, and Hiroshi Yamataka*

Department of Chemistry and Research Center for Smart Molecules, Rikkyo University, Nishi-Ikebukuro, Toshima-ku 171-8501 Tokyo, Japan

ABSTRACT: The Schmidt rearrangement of substituted 3-phenyl-2-butanone with trimethylsilyl azide in 90% (v/v) aqueous TFA gave two types of product, fragmentation and rearrangement, the ratio of which depends on the substituent: more fragmentation for a more electron-donating substituent. Rate measurements by azotometry indicated the presence of an induction period, and the pseudo-first-order rate constants showed saturation kinetics with respect to the azide concentration. It was indicated that the reaction proceeds through pre-equilibrium in the formation of iminodiazonium (ID) ion and that the N_2 liberation from the ID ion is rate-determining. Under high azide concentration conditions, where the effective reactant is the ID ion, the reaction gave a linear Hammett plot with a ρ value of −0.50. The observed substituent effects on the rate and the product selectivity imply that path bifurcation on the way from the rate-determining TS to the product states occurs, as suggested by previous molecular dynamics simulations, in a similar manner to the analogous Beckmann rearrangement/fragmentation reactions.

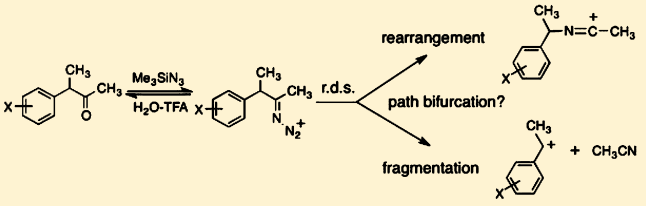

INTRODUCTION

The Schmidt and Beckmann rearrangements are well-known rearrangement reactions at an electron-deficient nitrogen center.[1] Both reactions give a carboxylic acid amide from a ketone. However, the reaction mechanism is much less known for the Schmidt compared with the Beckmann rearrangement.

The reaction pathway of the Schmidt rearrangement is often written as eq 1, in which azidohydrin (AH) and iminodiazonium ion (ID) are important intermediates. Although there has been a claim that an amide is directly formed from AH,[2] ID is commonly considered to be the precursor intermediate for the rearrangement.[3−6] The reaction of $PhCH{=}C(CH_3)N_3$ under acidic conditions was shown to give a mixture of $PhCH_2$- and CH_3-migrated amides, whose ratio was the same as that observed for the Schmidt reaction of $PhCH_2COCH_3$. The results indicated that ID ($PhCH_2C(CH_3)N_3^+$) was the common intermediate of the two reactions.[5]

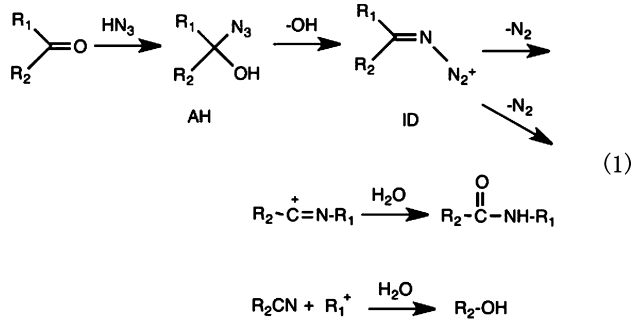

(1)

Product analysis studies for the Schmidt reactions of ketones, ArCOR, showed that the fraction of R rearrangement increased with the steric bulk of R,[3,4] which suggested that syn−anti isomerization in ID was slow and that a group located anti to N_2 migrated preferentially. The effect of substituent on the product ratio for the reactions of substituted benzophenones was reported to be small,[5] and information on the rate-determining step of the reaction is scarce. No kinetic measurement was carried out that allows one to analyze substituent effects. In another mechanistic aspect, the Schmidt rearrangement of ketones and aldehydes is known to yield fragmentation products (R^1 cation + R^2-CN) in addition to the expected rearrangement products, depending on the R^1 group in eq 1,[6,7] in an analogous way to the Beckmann reaction of ketoximes.[8−10] Previous computational study on the Schmidt reaction revealed that dynamic path bifurcation may occur, depending on the structure of the ketone, for the N_2-liberation step of ID, in which both rearrangement and fragmentation products are formed through a common transition state (TS).[11]

In the present study, we have carried out a kinetic and product analysis experiment to clarify important, but still unsolved, mechanistic issues for the Schmidt rearrangement: (1) identification of the rate-determining step of this multistep reaction, (2) substituent effects on the reactivity and product selectivity, (3) factors that determine the product ratio, and (4) possible occurrence of dynamic path bifurcation on the rearrangement/fragmentation step.

Received: February 28, 2012
Published: April 10, 2012

   dx.doi.org/10.1021/jo300419c | J. Org. Chem. 2012, 77, 4073−4078

RESULTS AND DISCUSSION

Product Analysis. Reactions of ring-substituted-3-phenyl-2-butanones, **1-X** (X = *p*-MeO, *p*-Me, *m*-Me, H, *p*-Cl, *m*-Cl, *p*-NO_2), with trimethylsilyl azide (TMSA) were carried out in 90% (v/v) aqueous TFA (eq 2). Since it became clear that the

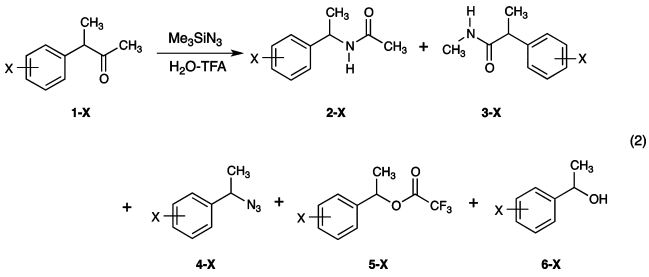

(2)

initial fragmentation product, **4-X**, underwent secondary reactions (vide infra), the product yields and the material balance were examined by analyzing the product distribution at less than 50% conversion of reaction. The products were identified and the yields were determined by ^{1}H NMR, and the results are listed in Table 1. The observed material balance was acceptable despite possible disturbance due to secondary reactions. It is clear that the product distribution depends strongly on the electronic nature of the substituent. The major product was the rearrangement product, **2-X** for X = *m*-Cl and *p*-CF_3, but the fragmentation product, **4-X**, became a major product for **1-X** with an electron-donating X. Another fragmentation product, **6-X**, could not be detected. It was considered to be possible that the nitrilium ion (R_2–C^+=N–R_1) intermediate is trapped by N_3^- and subsequent R_2 rearrangement and hydrolysis give the dialkylurea derivative ($R_2NHCONHR_1$). Actually, however, this type of product was not obtained.

Rate Measurement. *UV Spectrometry.* Attempted measurements of rate constants of the Schmidt reactions of **1-X** were carried out photometrically in 90% (v/v) TFA at 30 °C. For **1-H**, the absorbance at 299 nm increased monotonically up to 24 min, and then started to decrease, as illustrated in Figure 1. The time dependence of the UV absorbance for *p*-Me, H, and *p*-CF_3 derivatives (Figure 2) suggested the formation and decomposition of some kind of intermediate during the course of the reaction, especially for X = *p*-Me and H. The time course of the absorbance did not allow the measurement of the rate constants of these reactions by the UV method.

Azotometry. The rate of N_2 evolution from the reaction mixture was monitored by using a gas buret for the reactions of **1-X** (X = *p*-MeO, *p*-Me, *m*-Me, H, *p*-Cl, *m*-Cl, and *p*-CF_3) with TMSA in 90% (v/v) TFA at 0 °C. Two representative N_2 evolution–time plots are shown in Figure 3. Two points are apparent in Figure 3. First, in both cases, the evolution of N_2 did not start right after the reaction was allowed to occur by mixing the ketone and TMSA and showed an induction period. Second, the plot exhibited different patterns depending on the substituent. The plot for X = *p*-CF_3 was normal, in which the infinity value of evolved N_2 agreed with the theoretical one calculated from the initial concentration of the ketone ([**1-*p*-CF_3**] = 0.05 M, 90% (v/v) TFA, 6.0 mL). The data gave good linear pseudo-first-order kinetic plots, if the induction period observed at the very beginning of the reaction was neglected. On the other hand, the reaction of **1-*m*-Me** produced more N_2 than expected from the ketone concentration. Apparently, additional N_2 was generated from a secondary reaction in addition to the Schmidt reaction of the ketone and TMSA. The additional N_2 generation became more significant when X was more electron-donating.

It appeared reasonable to expect that fragmentation product **4-X** underwent further reactions to generate N_2. The reaction of separately prepared **4-H** at 0 °C in 90% (v/v) TFA indeed generated N_2 and yielded *N*-1-phenylethylaniline as the major product, probably through the route in Scheme 1. The reaction of **4-H** in 90% (v/v) TFA at 25 °C exhibited the time-dependent UV spectra (Figure 4), which were similar to those observed for the Schmidt reaction of **1-H** in Figure 1. The fact strongly suggested that the UV spectrum observed during the course of the Schmidt reaction was due to α-phenylethyl cation.[12,13]

Pseudo-first-order kinetic analyses of the results of the azotometry experiment were made by using data of the 1.0–2.0 mL N_2-evolution period (14–28% conversion of reaction) for each substituted derivative in order to avoid interference from the initial induction and the secondary reactions. Although the absolute rate constants could be in significant error because of the arbitrary selection and the narrow range of data points used in the kinetic analyses, the relative reactivities would be much more reliable since the analyses were made in the same way for all substituted derivatives.

Effect of TMSA Concentration. Rate measurements by azotometry at different TMSA concentrations were carried out for selected derivatives, and the results are listed in Table 2. The rate constants did not show a linear dependence on the TMSA concentration as required for the second-order kinetics, but showed the sign of saturation kinetics (Figure 5). The occurrence of saturation of the pseudo-first-order rate constants with the concentration of TMSA reflects the multistep nature of the Schmidt rearrangement/fragmentation reaction.

Substituent Effect. The observations of the saturation kinetics and the induction period suggested that the Schmidt

Table 1. Product Yields for the Reaction of 1-X and TMSA in 90% (v/v) TFA at 0 °C[a]

X	2-X	3-X	4-X	5-X	$F/(R+F)$[b]	material balance (%)
p-MeO	0	0	95 ± 1	5 ± 1	100	98
p-Me	0	5 ± 1	94 ± 1	1 ± 1	95	100
m-Me	3 ± 1	5 ± 1	87 ± 1	5 ± 1	92	95
H	10 ± 3	5 ± 1	79 ± 1	6 ± 3	85	92
p-Cl	16 ± 1	7 ± 1	67 ± 1	10 ± 1	77	98
m-Cl	87 ± 1	3 ± 1	8 ± 1	2 ± 1	10	91
p-CF_3	92 ± 1	8 ± 1	0	0	0	99

[a]Initial concentration: [**1-X**] = 0.05 M, [TMSA] = 0.50–1.0 M. Yields are relative yields in percentage, and material balance is based on the amount of remaining reactant and the absolute yields of the products. [b]Percentage of the fragmentation products over the total products.

dx.doi.org/10.1021/jo300419c | J. Org. Chem. 2012, 77, 4073–4078

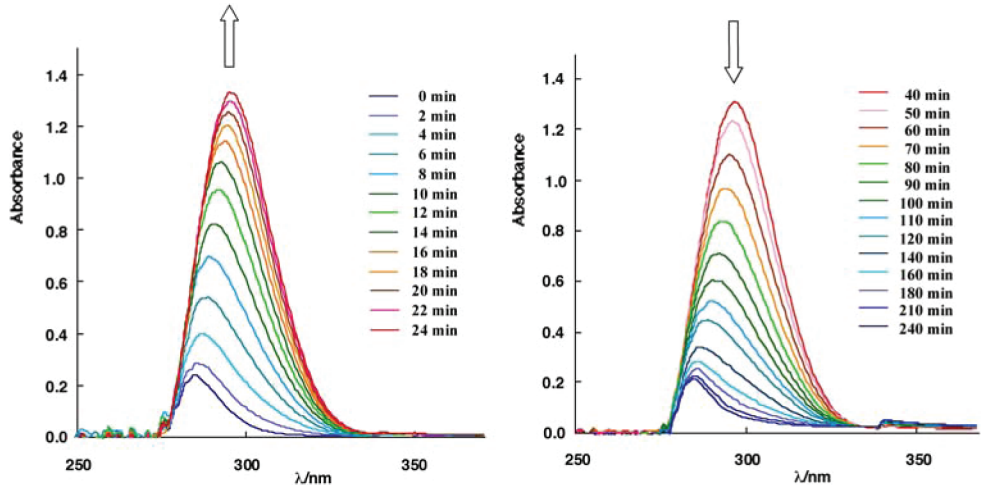

Figure 1. Time dependence of UV spectra for the reaction of **1-H** and TMSA in 90% (v/v) TFA at 30 °C. [**1-H**] = 0.75 mM, [TMSA] = 150 mM.

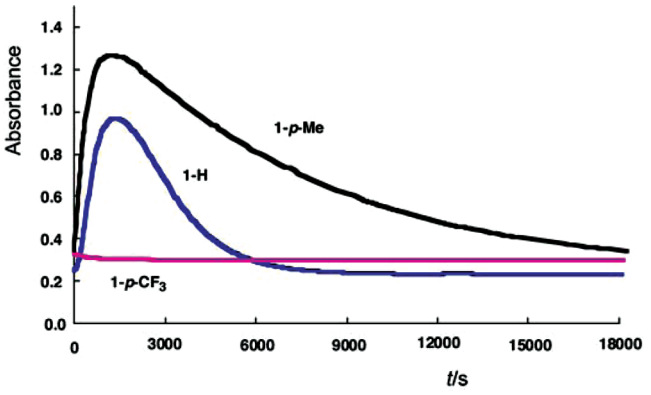

Figure 2. Time dependence of the absorbance at 299 nm for **1-X** (X = *p*-Me, H, *p*-CF_3) at 30 °C. [**1-H**] = 0.75 mM, [TMSA] = 150 nM in 90% (v/v) TFA.

rearrangement obeys pre-equilibrium kinetics. The reaction is initiated by carbonyl addition of N_3^- to give AH. Dehydration from AH to ID is expected to be fast in TFA, and hence the kinetic scheme is expressed by eq 3 and the kinetic equation is

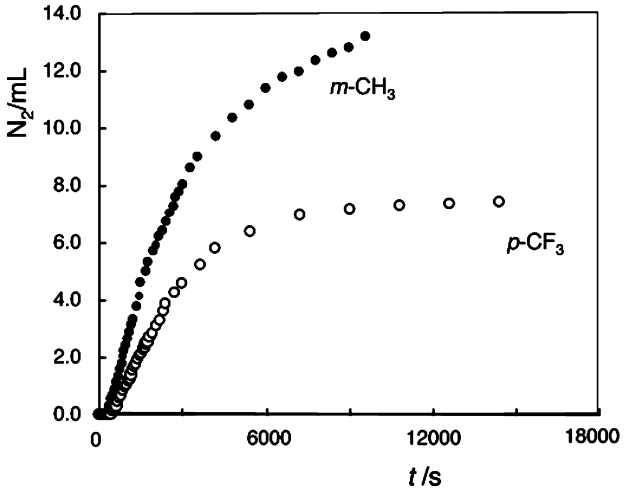

Figure 3. Time dependence of N_2 evolution for the reaction of **1-X** (0.05 M) and TMSA (0.50 M) at 0 °C. Closed circle for X = *m*-Me and open circle for X = *p*-CF_3.

Scheme 1

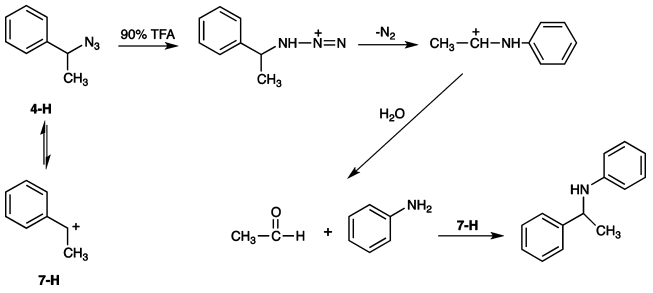

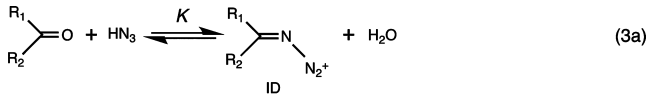

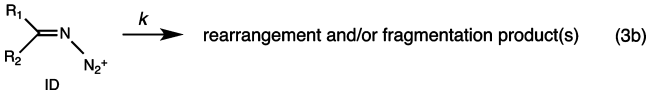

given by eq 4. According to this mechanism, the observed rate constant is first-order with respect to the azide concentration at low [TMSA] and zero-order at high [TMSA]. Under high azide concentration conditions, where the reaction gives the zero-order kinetics with respect to [TMSA], the ID ion acts as the effective reactant since the equilibrium in eq 3a lies on the ID side, and the N_2-liberation step becomes rate-determining. The pseudo-first-order rate constants at a [TMSA] of 1.50 M were then measured for all substituted derivatives and are listed in Table 3. The Hammett plot gave a ρ value of −0.50 (Figure 6). The point for *p*-MeO deviates downward from the correlation line, partly because of a decreased electron-donating ability of *p*-MeO in the highly acidic medium and because of an exalted resonance stabilization of ID compared to that in the TS (Chart 1, vide infra). It is interesting to note here that the ρ value is much smaller than that for the Beckmann rearrangement, despite the fact that the N_2- or H_2O-liberation step is considered rate-determining in both cases.

$$k_{obs} = Kk[N_3^-]/(1 + K[N_3^-]) \quad (4)$$

Previous computational studies on the Schmidt and the Beckmann rearrangement of ketone **1-X** showed that the ρ

dx.doi.org/10.1021/jo300419c | J. Org. Chem. 2012, 77, 4073−4078

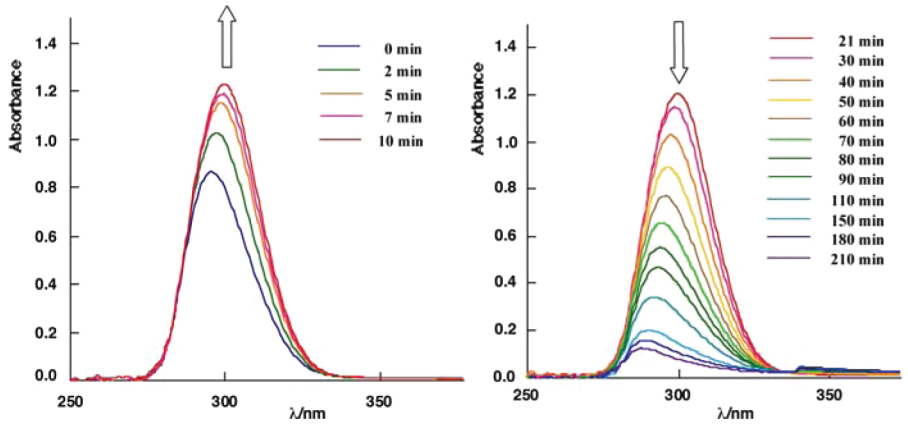

Figure 4. Time dependence of UV spectra for the reaction of **4-H** in 90% (v/v) TFA at 25 °C. [**4-H**] = 0.75 mM.

Table 2. Pseudo-First-Order Rate Constant ($10^4 k_{obs}/s^{-1}$) Determined by Azotometry for the Reaction of 1-X at Different TMSA Concentrations in 90% (v/v) TFA at 0 °C[a]

X	0.20[b]	0.375[b]	0.50[b]	0.75[b]	1.00[b]	1.20[b]	1.50[b]
p-MeO	1.92 ± 0.14	3.16 ± 0.33	3.68 ± 0.19	3.95 ± 0.21	3.93 ± 0.36	4.34 ± 0.06	4.37 ± 0.26
H	1.75 ± 0.14	2.40 ± 0.46	2.69 ± 0.37	3.44 ± 0.30	3.58 ± 0.15	3.77 ± 0.07	3.79 ± 0.31

[a]Initial concentration of [**1-X**] is 0.05 M. Rate constants are the average of 4-7 measurements, and errors are standard deviations. [b]Concentration of TMSA in M.

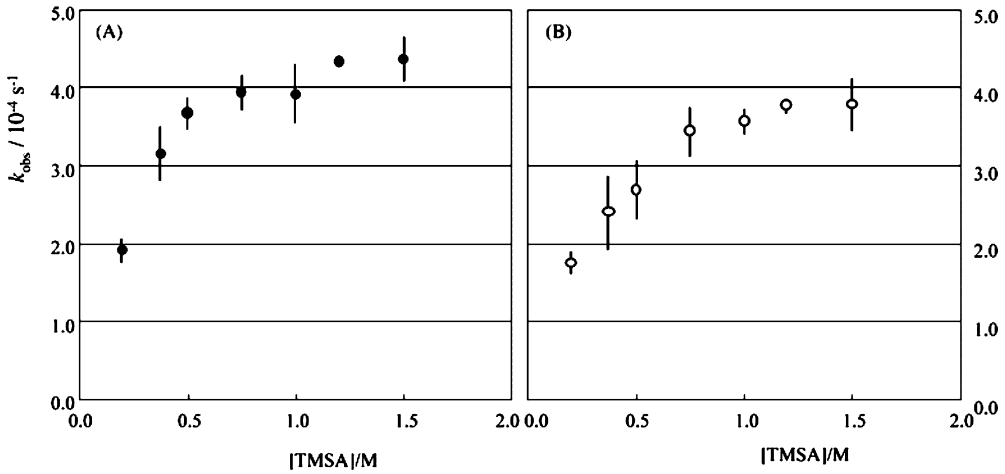

Figure 5. Concentration dependence of the pseudo-first-order rate constants for the Schmidt reactions of (A) **1-*p*-OMe** and (B) **1-H** in 90% (v/v) TFA at 0 °C. The initial concentration of **1-X** = 0.05 M.

Table 3. Pseudo-First-Order Rate Constant ($10^4 k_{obs}/s^{-1}$) Determined by Azotometry for the Reaction of 1-X at [TMSA] = 1.50 M in 90% (v/v) TFA at 0 °C[a]

	p-MeO	*p*-Me	*m*-Me	H	*p*-Cl	*m*-Cl	*p*-CF_3
$10^4 k_{obs}/s^{-1}$	4.37 ± 0.26	4.86 ± 0.44	4.04 ± 0.27	3.79 ± 0.31	2.95 ± 0.29	2.62 ± 0.28	2.11 ± 0.22

[a]Initial concentration of [**1-X**] is 0.05 M. Rate constants are the average of 4−7 measurements, and errors are standard deviations.

values for N_2 liberation from ID (Schmidt) and H_2O liberation from oxime (Beckmann) are large (−7.1) for the Beckmann[9] and near zero for the Schmidt reaction.[11] The experimental ρ value for Beckmann was −2.2.[10] Thus, the present small ρ value is in line with the computational prediction. The reason for the small ρ value for the Schmidt rearrangement step is that the unit positive charge on the ID ion is delocalized into the phenyl ring, as shown in Chart 1, which makes the stability of the ID ion substituent-dependent. The significant substituent effect in the effective reactant masked the substituent effect on the TS stability, and hence the Hammett ρ value on the process from ID to TS became small, as observed. The rationale was supported by previous MO calculations.[11]

It should be noted that the Hammett plots in Figure 6 gave a reasonably good straight line. This indicates that the reaction mechanism is the same for all substituted derivatives, whereas the product distribution (rearrangement vs fragmentation) is different with substituent. If the two products are formed via independent and concurrent paths, a change of relative importance of the two paths should have given V-shaped Hammett plots, which were not observed. To further examine the possibility of the concurrent mechanism, the observed rate

dx.doi.org/10.1021/jo300419c | J. Org. Chem. 2012, 77, 4073−4078

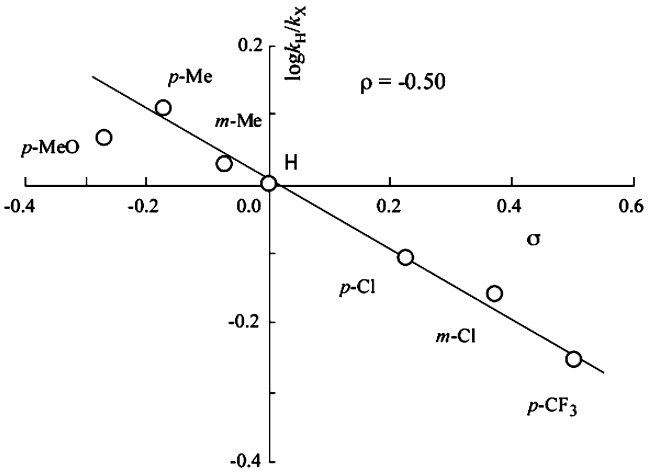

Figure 6. Hammett plot for the Schmidt reaction of **1-X** in 90% (v/v) TFA at 0 °C. The initial concentration of [**1-X**] = 0.05 M, and [TMSA] = 1.50 M.

Chart 1

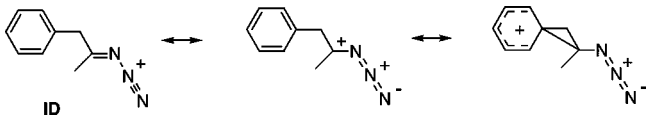

constants were divided into individual rate constants, k_r and k_f, for the rearrangement and fragmentation steps, respectively, under the assumption that the two types of products were formed from ID directly and independently. The calculated k_r and k_f were then used to construct Hammett plots in Figure 7.

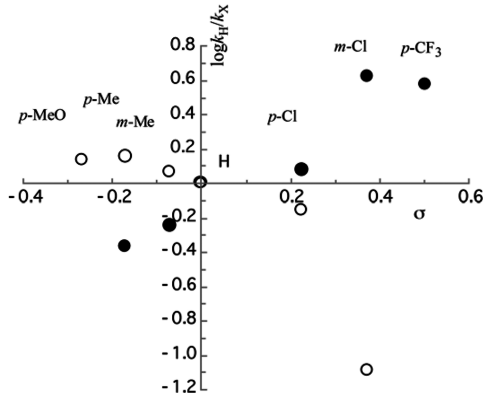

Figure 7. Hammett plots for the rearrangement (filled circle) and fragmentation (open circle) steps of the Schmidt reaction of **1-X** in 90% (v/v) TFA at 0 °C. Rate constants for each step were derived under the assumption that the rearrangement and fragmentation steps are independent and concurrent pathways. The initial concentration of [**1-X**] = 0.05 M, and [TMSA] = 1.50 M.

Apparently, both Hammett plots showed poor correlation against the standard σ constants. Furthermore, the plot for the rearrangement gave a positive slope, which is inconsistent with the step. Thus, the Hammett plots in Figure 6 strongly argued the concurrent product formation mechanism unlikely.

In the Beckmann reaction, MO calculations gave a linear Hammett plot for the H_2O-liberation step together with a strong substituent dependence on the product distribution. Molecular dynamics (MD) simulations indicated that the apparent discrepancy between substituent effects on the rate and the product selectivity could arise from path bifurcation occurring on the way from the TS to the products.[9] Experimental results on the Beckmann reaction agreed with the MO predictions on the substituent effects on the rate and the product selectivity and gave support for the computational predictions of path bifurcation.[10]

In the Schmidt reaction, MO calculations gave a small ρ value for the N_2-liberation step and MD simulations indicated path bifurcation occurring on the way from the TS to the products,[11] in a similar manner to the Beckmann reaction. The present experimental results on the Schmidt reaction agreed with the MO calculations on the substituent effects on the rate and the product selectivity, and thus it is likely that a path bifurcation on the way from the TS to product states occurs for the Schmidt reaction of **1-X** as well in a similar manner to the Beckmann reaction.

SUMMARY AND CONCLUDING REMARKS

Analysis of the Schmidt rearrangement of **1-X** was complicated by the secondary reaction of initially formed fragmentation products. Nevertheless, kinetic measurements by means of azotometry revealed two important features: the presence of an induction period, and saturation kinetics with respect to azide concentrations. It was indicated that the reaction proceeds through pre-equilibrium in the formation of the ID ion and that the N_2 liberation from the ID ion could be rate-determining. The effective reactant is the ID ion under high azide concentration conditions. The reaction gave linear Hammett plots with a ρ value of −0.50. The small ρ value is consistent with the mechanism. The reaction gave two types of products, fragmentation and rearrangement, the ratio of which depends on the substituent: more fragmentation for a more electron-donating substituent. The analysis of the observed substituent effects on the rate and the product selectivity eliminates the mechanism of concurrent reaction pathways. A plausible mechanism is that path bifurcation on the way from the rate-determining TS to the product states occurs in the Schmidt rearrangement, as suggested by previous MD simulations in a similar manner to the analogous Beckmann rearrangement. It should be noted that such bifurcation was observed for a specially designed system, which reacts in a borderline mechanism and gives two products in different ratios depending on substituent. Thus, the present results do not necessarily suggest the occurrence of bifurcation for commonly used substrates, but it is sure that the possibility of path bifurcation should be taken into consideration when a reaction mechanism and a product selectivity are in question.

EXPERIMENTAL METHODS

Materials. 1-Substituted-phenyl-2-propanones were synthesized from corresponding benzaldehydes by nitroaldol with $EtNO_2$,[14] and Fe reduction.[15] 3-Substituted-phenyl-2-butanones (**1-X**) were prepared from 1-substituted-phenyl-2-propanones by methylation (MeI/NaOH) and purified by using 2,4-dinitrophenylhydrazine. Hydrolyses of hydrazones gave nearly pure **1-X**, which were further purified by distillation, and column chromatography (hexane/AcOEt = 4:1). Reaction solvents were purified by distillation. Trimethylsilyl azide was used as received.

3-*p*-Methoxyphenyl-2-butanone 2,4-Dinitrophenylhydrazone: ^{1}H NMR ($CDCl_3$, 400 MHz) δ 11.1 (s, 1H), 9.15 (d, J = 2.9 Hz, 1H), 8.35 (dd, J = 9.6, 2.9 Hz, 1H), 8.06 (d, J = 9.6 Hz, 1H), 7.16 (d, J = 8.6 Hz, 2H), 6.88 (d, J = 8.6 Hz, 2H), 3.80 (s, 3H), 3.76 (q, J = 7.2 Hz, 1H), 1.90 (s, 3H), 1.54 (d, J = 7.2 Hz, 3H). mp 129−134 °C.

dx.doi.org/10.1021/jo300419c | J. Org. Chem. 2012, 77, 4073−4078

3-*p*-Methylphenyl-2-butanone 2,4-Dinitrophenylhydrozone: ^{1}H NMR ($CDCl_3$, 400 MHz) δ 11.1 (s, NH), 9.15 (d, J = 2.4 Hz, 1H), 8.35 (dd, J = 9.6, 2.4 Hz, 1H), 8.07 (d, J = 9.6 Hz, 1H), 7.12−7.18 (m, 4H), 3.78 (q, J = 7.0 Hz, 1H), 1.91 (s, 3H), 1.54 (d, J = 7.0 Hz, 3H). mp 129−134 °C.

3-*m*-Methylphenyl-2-butanone 2,4-Dinitrophenylhydrozone: ^{1}H NMR ($CDCl_3$, 400 MHz) δ 11.1 (s, NH), 9.16 (d, J = 2.8 Hz, 1H), 8.36 (dd, J = 9.6, 2.8 Hz, 1H), 8.08 (d, J = 9.6 Hz, 1H), 7.04−7.25 (m, 4H), 3.77 (q, J = 7.3 Hz, 1H), 2.35 (s, 3H), 1.91 (s, 3H), 1.55 (d, J = 7.3 Hz, 3H). mp 146−147 °C.

3-Phenyl-2-butanone 2,4-Dinitrophenylhydrozone: ^{1}H NMR ($CDCl_3$, 400 MHz) δ 11.1 (s, NH), 9.15 (d, J = 2.9 Hz, 1H), 8.35 (dd, J = 9.6, 2.9 Hz, 1H), 8.07 (d, J = 9.6 Hz, 1H), 7.24−7.35 (m, 5H), 3.82 (q, J = 6.9 Hz, 1H), 1.92 (s, 3H), 1.57 (d, J = 6.9 Hz, 3H). mp 169−171 °C.

3-*p*-Chlorophenyl-2-butanone 2,4-Dinitrophenylhydrozone: ^{1}H NMR ($CDCl_3$, 400 MHz) δ 11.1 (s, NH), 9.15 (d, J = 2.3 Hz, 1H), 8.36 (dd, J = 9.6, 2.3 Hz, 1H), 8.04 (d, J = 9.6 Hz, 1H), 7.32 (d, J = 8.6 Hz, 2H), 7.19 (d, J = 8.6 Hz, 2H), 3.79 (q, J = 6.9 Hz, 1H), 1.91 (s, 3H), 1.55 (d, J = 6.9 Hz, 3H). mp 114−116 °C.

3-*m*-Chlorophenyl-2-butanone 2,4-Dinitrophenylhydrozone: ^{1}H NMR ($CDCl_3$, 400 MHz) δ 11.1 (s, NH), 9.16 (d, J = 2.4 Hz, 1H), 8.36 (dd, J = 9.6, 2.4 Hz, 1H), 8.05 (d, J = 9.6 Hz, 1H), 7.13−7.31 (m, 4H), 3.79 (q, J = 7.0 Hz, 1H), 1.92 (s, 3H), 1.56 (d, J = 7.0 Hz, 3H). mp 130−134 °C.

3-*p*-Trifluoromethylphenyl-2-butanone 2,4-Dinitrophenylhydrozone: ^{1}H NMR ($CDCl_3$, 400 MHz) δ 11.1 (s, NH), 9.15 (d, J = 2.8 Hz, 1H), 8.36 (dd, J = 9.8, 2.8 Hz, 1H), 8.04 (d, J = 9.8 Hz, 1H), 7.61 (d, J = 8.4 Hz, 2H), 7.38 (d, J = 8.4 Hz, 2H), 3.89 (q, J = 6.8 Hz, 1H), 1.93 (s, 3H), 1.59 (d, J = 6.8 Hz, 3H). The melting point was not measured since the sample was contaminated by the hydrazone of dimethylated ketone.

Substituted 3-phenyl-2-butanone (**1-X**) purified via hydrazone, distillation, and column chromatography showed >99% purity with GC, and their NMR spectra were consistent with those in the literature.[16]

3-*p*-Methoxyphenyl-2-butanone (1-*p*-MeO): ^{1}H NMR ($CDCl_3$, 400 MHz) δ 7.13 (d, J = 8.4 Hz, 2H), 6.87 (d, J = 8.4 Hz, 2H), 3.80 (s, 3H), 3.69 (q, J = 6.9 Hz, 1H), 2.04 (s, 3H), 1.36 (d, J = 6.9 Hz, 3H). bp 100−101 °C/0.7 Torr.

3-*p*-Methylphenyl-2-butanone (1-*p*-Me): ^{1}H NMR ($CDCl_3$, 400 MHz) δ 7.15 (d, J = 8.4 Hz, 2H), 7.10 (d, J = 8.4 Hz, 2H), 3.70 (q, J = 7.0 Hz, 1H), 2.33 (s, 3H), 2.04 (s, 3H), 1.37 (d, J = 7.0 Hz, 3H). bp 70 °C/0.5 Torr.

3-*m*-Methylphenyl-2-butanone (1-*m*-Me): ^{1}H NMR ($CDCl_3$, 400 MHz) δ 7.00−7.24 (m, 4H), 3.70 (q, J = 7.2 Hz, 1H), 2.34 (s, 3H), 2.05 (s, 3H), 1.37 (d, J = 7.2 Hz, 3H). bp 173−74 °C/0.5 Torr.

3-Phenyl-2-butanone (1-H): ^{1}H NMR ($CDCl_3$, 400 MHz) δ 7.21−7.36 (m, 5H), 3.74 (q, J = 7.0 Hz, 1H), 2.05 (s, 3H), 1.39 (d, J = 7.0 Hz, 3H). bp 65−66 °C/0.5 Torr.

3-*p*-Chlorophenyl-2-butanone (1-*p*-Cl): ^{1}H NMR ($CDCl_3$, 400 MHz) δ 7.31 (d, J = 8.2 Hz, 2H), 7.15 (d, J = 8.2 Hz, 2H), 3.73 (q, J = 7.1 Hz, 1H), 2.06 (s, 3H), 1.38 (d, J = 7.1 Hz, 3H). bp 80−85 °C/0.7 Torr.

3-*m*-Chlorophenyl-2-butanone (1-*m*-Cl): ^{1}H NMR ($CDCl_3$, 400 MHz) δ 7.09−7.28 (m, 4H), 3.72 (q, J = 7.0 Hz, 1H), 2.07 (s, 3H), 1.39 (d, J = 7.0 Hz, 3H). bp 73−74 °C/0.4 Torr.

3-*p*-Trifluoromethylphenyl-2-butanone (1-*p*-CF_3): ^{1}H NMR ($CDCl_3$, 400 MHz) δ 7.60 (d, J = 8.0 Hz, 2H), 7.35 (d, J = 8.0 Hz, 2H), 3.83 (q, J = 6.8 Hz, 1H), 2.08 (s, 3H), 1.42 (d, J = 6.8 Hz, 3H). bp 75 °C/0.4 Torr.

Product Analysis. Material balance and product distribution were determined by analyzing the reaction mixture by NMR. A mixture of **1-X** (0.05 M), TMSA (0.50 M), and a small amount of dibenzyl ether as an internal standard for NMR measurement was allowed to react at 0.0 ± 0.5 °C for a preset time. The reaction solution was poured into cold benzene, and the solvent was evaporated. The remaining material was dissolved in $CDCl_3$, and the NMR spectrum was recorded. The products were identified by comparing the spectra with those of separately prepared authentic samples, and the yields were determined by comparing proton intensities of the products and the internal standard.

Rate Measurements. Azotometry. A 90% (v/v) TFA solution of **1-X** (1.00 mmol, 10.0 mL) and a solution of TMSA (10.00 mol, 10.0 mL) were separately prepared at 0.0 ± 0.5 °C. Two solutions (3.0 mL each) were mixed by means of a hypodermic syringe in a two-neck flask connected to a gas buret, and the amount of gas evolved was measured volumetrically. After some induction period, gas evolution started, but for all **1-X**, except X = *p*-CF_3, the amount of N_2 evolved exceeded the theoretical value (7.3 mL) due to secondary reactions of fragmentation products. To avoid disturbance by the induction period and the secondary reactions, pseudo-first-order kinetics was analyzed by using a 1.0−2.0 mL range of N_2 evolution, which corresponds to the conversion of reaction of 14%−28%. Although the absolute rate constants could be in significant error because of the arbitrary selection and the narrow range of data used in the kinetic analyses, the relative reactivities would be much more reliable since the analyses were made in the same way for all substituted derivatives.

AUTHOR INFORMATION

Corresponding Author

*E-mail: yamataka@rikkyo.ac.jp.

Notes

The authors declare no competing financial interest.

ACKNOWLEDGMENTS

The study was, in part, supported by the SFR aid by Rikkyo University, and a Grant-in-Aid for Scientific Research from the Ministry of Education, Science, Sports, Culture and Technology, Japan.

REFERENCES

(1) Smith, P. A. S. In *Molecular Rearrangements*; de Mayo, P., Ed.; Wiley: New York, 1963; Vol. *1*, Chapter 8.

(2) Fikes, L. E.; Shechter, H. *J. Org. Chem.* **1979**, *44*, 741.

(3) Szmant, H. H.; McIntosh, J. J. *J. Am. Chem. Soc.* **1950**, *72*, 4835.

(4) Smith, P. A. S.; Horwits, J. P. *J. Am. Chem. Soc.* **1950**, *72*, 3718.

(5) Hassner, A.; Ferdinandi, E. S.; Isbister, R. J. *J. Am. Chem. Soc.* **1970**, *92*, 1672.

(6) Richard, J. P.; Amyes, T. L.; Lee, Y.-G.; Jagannadham, V. *J. Am. Chem. Soc.* **1994**, *116*, 10833.

(7) Amyes, T. L.; Richard, J. P. *J. Am. Chem. Soc.* **1991**, *113*, 1867.

(8) Grob, C. A.; Fischer, H. P.; Raudenbusch, W.; Zeŕgenyi, J. *Helv. Chim. Acta* **1964**, *47*, 1003.

(9) Yamataka, H.; Sato, M.; Hasegawa, H.; Ammal, S. C. *Faraday Discuss.* **2010**, *145*, 327.

(10) Yamamoto, Y.; Hasegawa, H.; Yamataka, H. *J. Org. Chem.* **2011**, *76*, 4652.

(11) Katori, T.; Itoh, S.; Sato, M.; Yamataka, H. *J. Am. Chem. Soc.* **2010**, *132*, 3413.

(12) Cozens, F. L.; Kanagasabapathy, V. M.; McClelland, R. A.; Steenken, S. *Can. J. Chem.* **1999**, *77*, 2069.

(13) Fujisaki, N.; Comte, P.; Gäumann, T. *J. Chem. Soc., Chem. Commun.* **1993**, 8.

(14) Miyano, S.; Hokari, H.; Hashimoto, H. *Bull. Chem. Soc. Jpn.* **1982**, *55*, 534.

(15) Hass, H. B.; Susie, A. G.; Heider, R. L. *J. Org. Chem.* **1950**, *15*, 8.

(16) (a) Fry, A. J.; Bujanauskas, J. P. *J. Org. Chem.* **1978**, *43*, 3157. (**1-*p*-MeO**). (b) Gompper, R.; Hans Huber, V. *Chem. Ber.* **1981**, *114*, 2866. (**1-*p*-MeO**, **1-*p*-Me**, **H**, **1-*p*-Cl**). (c) Liu, C.; He, C.; Shi, W.; Chen, M.; Lei, A. *Org. Lett.* **2007**, *9*, 5601. (**1-H**, **1-*p*-Cl**). (d) Rodríguez, C.; de Gonzalo, G.; Pazmiño, D. E. T.; Fraaije, M. W.; Gotor, V. *Tetrahedron: Asymmetry* **2009**, *20*, 1168 (**1-*m*-Me**, **1-*m*-Cl**).